



LAWRENCE  
LIVERMORE  
NATIONAL  
LABORATORY

# KCAT Performance Summary - Update, Rev 1

A. Waters, H. Martz, C. Logan, J. Gross, D. Chinn

September 15, 2004

## **Disclaimer**

---

This document was prepared as an account of work sponsored by an agency of the United States Government. Neither the United States Government nor the University of California nor any of their employees, makes any warranty, express or implied, or assumes any legal liability or responsibility for the accuracy, completeness, or usefulness of any information, apparatus, product, or process disclosed, or represents that its use would not infringe privately owned rights. Reference herein to any specific commercial product, process, or service by trade name, trademark, manufacturer, or otherwise, does not necessarily constitute or imply its endorsement, recommendation, or favoring by the United States Government or the University of California. The views and opinions of authors expressed herein do not necessarily state or reflect those of the United States Government or the University of California, and shall not be used for advertising or product endorsement purposes.

This work was performed under the auspices of the U.S. Department of Energy by University of California, Lawrence Livermore National Laboratory under Contract W-7405-Eng-48.

# KCAT Performance Summary – Update, Rev 1<sup>1</sup>

Amy Waters, Harry Martz, Clint Logan, Jeff Gross, and Diane Chinn

UCRL-TR-203519-REV-1

Lawrence Livermore National Laboratory

## Introduction

High Energy Density Physics (HEDP) experiments play an important role in corroborating the improved physics codes that underlie LLNL's Stockpile Stewardship mission. Conducting these experiments, whether on the National Ignition Facility (NIF) or another national facility such as Omega, will require not only improvement in the diagnostics for measuring the experiment, but also detailed knowledge of the as-built target components and assemblies themselves. To assist in this effort, a defined set of well-known reference standards designed to represent a range of HEDP targets have been built and are being used to quantify the performance of different characterization techniques. Without the critical step of using reference standards for qualifying characterization tools there can be no verification of either commercial or internally-developed characterization techniques and thus an uncertainty in the input to the physics code models would exist.

## Reference standards

In FY03, two reference standards were fabricated and characterized using metrology tools for this Engineering Technology Base project. One of the reference standards was built with a cylindrical geometry and contained features similar to those on a Super Nova Raleigh Taylor (SNRT) target. The other reference standard was built with a spherical geometry and contained features similar to those on a double shell target. The standards were designed for manufacturability, stability and to provide a range of features that can be measured using NDE methods.

## Digital radiography system performance

In an attempt to begin characterizing the reference standards, we have acquired data nondestructively using different x-ray digital radiography (DR) and computed tomography (CT) systems. Reports are being written to determine the performance of each DR/CT system investigated and used to characterize these reference standards. Here we present the report on LLNL's KCAT system.

Data from the reference standards was acquired using KCAT, a modular DR and CT system designed at LLNL. KCAT is a higher resolution system that utilizes a 160-kV polychromatic Kevex X-ray tube with a tungsten target. The full cone-angle for these acquisitions was  $\sim 1.3^\circ$ . KCAT employs a terbium-doped scintillating glass, optically coupled to a 1536 x 1024 CCD

---

<sup>1</sup> This work was performed under the auspices of the U. S. Department of Energy by the University of California Lawrence Livermore National Laboratory under contract No. W-7405-Eng-48.

camera with 14-bit digital resolution for detection of x-ray intensity. The pixel size of the camera is  $9\ \mu\text{m}$ .

During scans, the DR MTF edge (described below) and reference standards were placed approximately 54 mm from the X-ray source, and approximately 106 mm from the detector. This resulted in a geometric magnification of around three, with a resulting pixel size at the object of around  $3\ \mu\text{m}$ . The optimum energy appropriate for DR and CT of these reference standards was determined to be  $\sim 8\ \text{keV}$ . To approximate this energy for DR/CT we employed an electron tube voltage of 60 kV, with a current of 0.08 mA. For each projection image, two frames of 300-second integration times each were averaged for a total of 360 projections acquired over a  $360^\circ$  angular range. Total CT data acquisition time was approximately 60 hours.

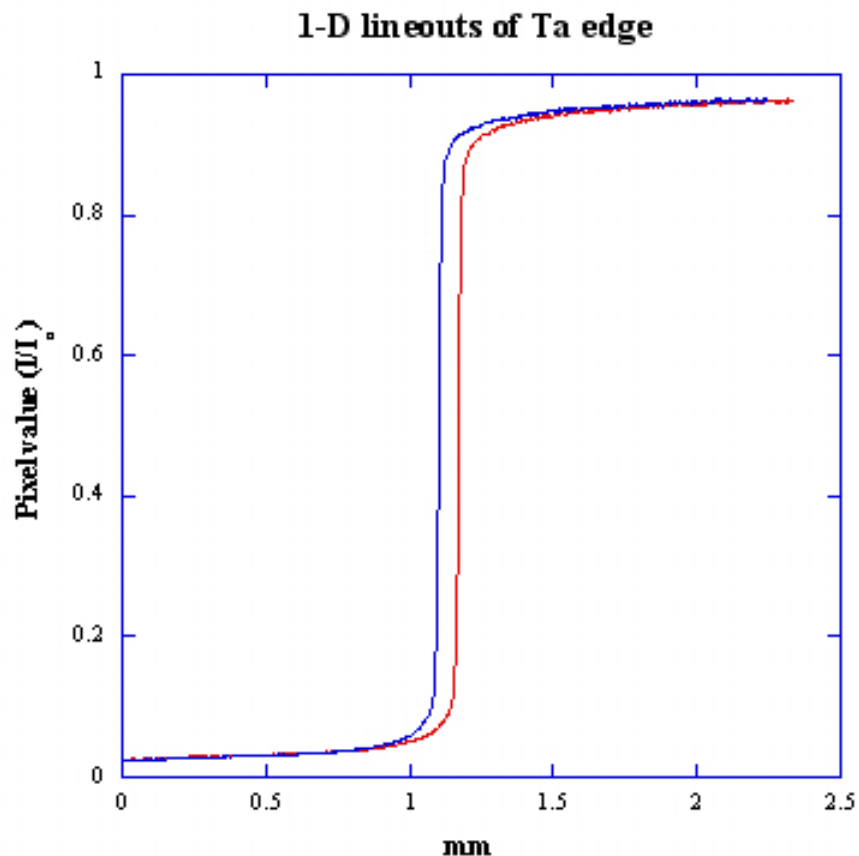


**Figure 1.** Two 10-pixel wide one-dimensional lineouts were taken from the thin tantalum edge transmission image. Two lineouts were used to calculate MTF to demonstrate repeatability of this technique.

In order to begin quantifying digital radiography system performance, a thin (0.51 mm) polished tantalum edge was imaged using identical DR/CT data acquisition parameters. Transmission images ( $I/I_0$ ) were created and a 10-pixel wide one-dimensional lineout was taken from the polished edge to determine the edge response of the system. Two lineouts taken from different areas of the Tantalum edge image are shown in Figure 1. Note there is a slight gradient in the lineouts far from the edge and the  $I_0$  values never reach a value of 1. This may be due to poor x-ray and light control. A better collimation system around the scintillator to decrease the excess light field may improve this situation.

The one-dimensional lineouts were used to measure the projection or DR Modulation Transfer Function (MTF) of the system. To calculate the MTF for the KCAT system, the derivative of the line-out (edge response) was calculated, resulting in what is called the edge-spread function. The Fourier transform of the edge-spread function is the line-spread MTF. The MTF is a frequency-domain description of the spatial resolution of an imaging system or component [Hasegawa 1991, Logan, et al. 1998]. The MTF of a system is the product of the MTFs of each of the components individually, and thus is a preferred characterization technique for many imaging experts. The MTF of a system is usually presented as a graph with frequency in  $\text{mm}^{-1}$ , or linepairs per millimeter (lp/mm) on the horizontal, or x-axis. At low spatial frequencies, the MTF usually approaches 1. The MTF falls with increasing frequency, and can never exceed a sinc function  $[\sin(x)/x]$ , where  $x$  is the pixel size. Modulation as a function of frequency in lp/mm is presented in Figure 2.

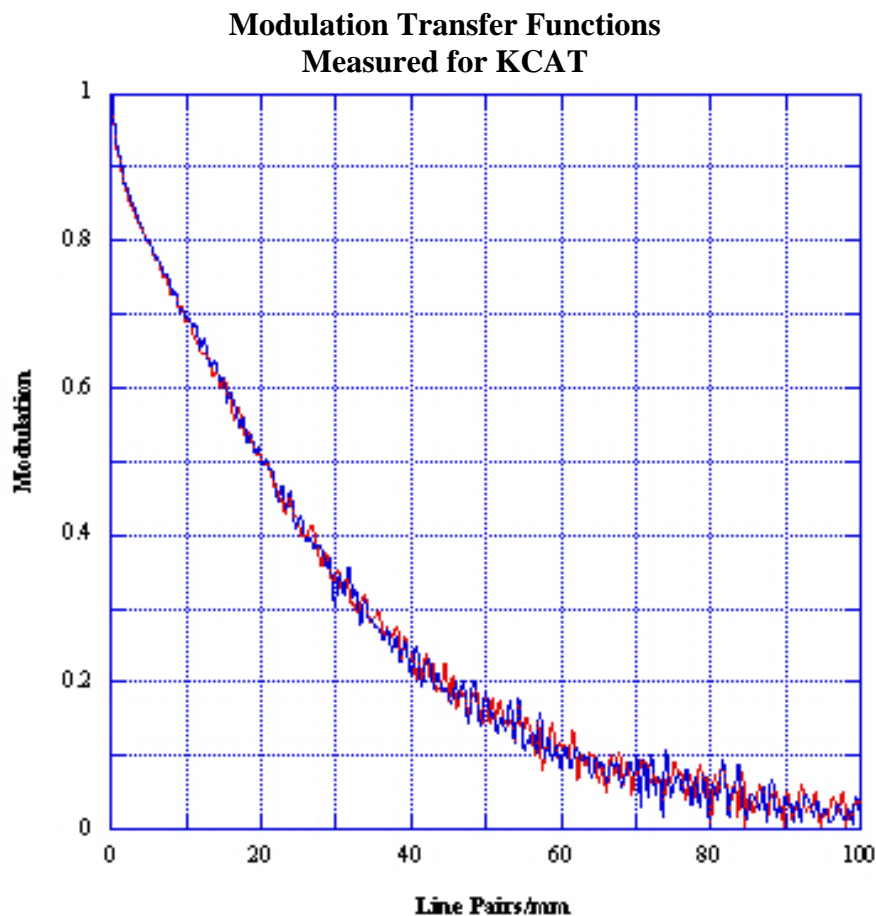


**Figure 2.** Two MTFs calculated for the KCAT system using the two lineouts shown in Figure 3. At 20 lp/mm, the modulation is ~50%.

Modulation can also be measured at a discrete frequency from a projection image of a linepair gauge. The commercial linepair gauge available to us has a maximum frequency of 20 lp/mm. The design of the gauge does not allow observation of low spatial frequencies within a single image at this small field of view. We can however observe a fiducial marker indicating 20 lp/mm. The thickness of the fiducial line is 3.5 times the thickness of the 20 lp/mm lines,

resulting in an equivalent frequency of 5.7 lp/mm. To measure MTF with this linepair gauge, a lineout was taken from the fiducial line and through the 20 lp/mm region. The ratio of the modulation of the 20 lp/mm to the modulation of the thicker fiducial line was then measured. Using this technique, at 20 lp/mm the modulation was 68% of the modulation at 5.7 lp/mm. The ratio of 68% between 20 lp/mm to 5.7 lp/mm measured on the line pair gauge agrees with the ratio shown in Figure 2 above. In other words, the MTF measured with the Ta edge and shown in Figure 2 shows the modulation at 20 lp/mm is approximately 68% of the value at 5 lp/mm.

To determine spatial resolution, one commonly used rule of thumb is to multiply the pixel size at the object by a factor of 2.5. Using this simple estimate of the spatial resolution, for the parameters described above the resulting spatial resolution of the KCAT system is approximately 7.5  $\mu\text{m}$ . Another quick and easy way to get a sense of the spatial resolution of a system is to fit the edge-spread function (calculated as the derivative of the one-dimensional lineout) with a Gaussian. The resulting Full Width Half Maximum (FWHM) of the Gaussian can be multiplied by the pixel size at the object to give an indication of “worst-case” system resolution. For the KCAT system, the FWHM of the Gaussian-fit edge-spread function was calculated to be 4.1, indicating a worst-case system spatial resolution of approximately 12.3  $\mu\text{m}$ .

Other techniques exist to quantify system performance, such as the Signal to Noise Ratio (SNR). The SNR is defined as the difference between the mean of two signals (in our case the two signals are within the Ta edge, and outside the Ta edge) divided by the square root of the sum of the squares of the standard deviation:

$$\frac{S_1 - S_2}{\sqrt{\sigma_1^2 + \sigma_2^2}},$$

where  $S$  is the mean of the signal and  $\sigma$  is the standard deviation of the signal.

The SNR of the DR of the tantalum edge can be calculated using the one-dimensional line-outs taken from the tantalum edge transmission image, and can also be calculated over an area (two-dimensions) (for both calculations  $S_1$  is defined as the mean within the Ta edge and  $S_2$  is defined as the mean far from the edge). For KCAT, the one-dimensional DR SNR of the Ta edge was calculated to be 74.3. The two-dimensional DR SNR of the Ta edge was determined for an area of 162 x 141 pixels, and was calculated to be 211.4.

Several preprocessing steps were necessary before the DR projections could be reconstructed into a CT volume. Each projection image was first converted into ray sums, or attenuation radiographs [ $\ln(I_0/I)$ ], and outlying pixels were removed using a median filter comparison algorithm. Attenuation is a function of material density, elemental composition, x-ray energy and path length through the material. Thus, in the resulting attenuation digital radiographs as displayed here, darker regions indicate lower attenuating materials and/or shorter path lengths, while lighter areas indicate higher attenuating materials and/or longer path lengths.

## **CT Data**

After creating attenuation radiographs, detector imbalances were minimized to avoid ring artifacts in the reconstructed images. Due to the size of the cone-angle ( $\sim 1.3^\circ$ ), it was determined that a cone-beam approximating reconstruction algorithm was the most appropriate to use with these data, and the set of 360 attenuation radiographs was finally reconstructed into a CT volume using a Feldkamp cone-beam reconstruction algorithm. The resulting CT volume may then be sliced along any designated orthogonal axes for analysis.

Much work needs to be done to quantify the CT data. Any quantified data resulting from this project must be relevant to the target design and fabrication communities. To this end we are working with those groups to identify data of interest. The information that has been determined to be of interest for the reference standards includes: qualitatively identifying flaws such as voids, and the wicking of glue; determining distributions of identified flaws, including maximum volumes, total number, and volume fractions; measuring concentricity; quantifying wall thicknesses, including the mean and standard deviations; measuring uniformity and voids within the bond; and measuring the interfaces between materials.

In addition, we are working to design and build additional objects that can be used to further quantify DR and CT system performance. A new edge has been designed and manufactured to more suitably measure the edge response functions and subsequently the MTFs for radiographs for the different DR/CT systems. Also, we are investigating ways to calculate the MTFs for CT images from existing data. To support this effort, a series CT MTF phantoms have been fabricated from tubes of different materials.

## **As-built models from CT data**

Characterization of the reference standard by X-ray CT reveals valuable information about the geometry and assembly of the subcomponents. Although some metrology is performed during fabrication, the state of the final product can only be identified through nondestructive characterization techniques. The X-ray CT images of the reference standards show that the geometry of the reference standards deviates from the design e.g. spherical shapes are not perfectly spherical and glue surfaces are uneven.

The performance of an object as it was built, as opposed to as it was designed, can be simulated by performing an analysis of an “as-built” model. A conventional simulation of the object uses the geometry found in the fabrication drawings in its model. This “ideal” model simulates the object under ideal fabrication conditions. In contrast, an “as-built” model uses the geometry derived from X-ray computed tomography to simulate the object under “as-built” conditions. Using an “as-built” model results in simulations under more realistic conditions, and includes any manufactured flaws, defects or anomalies.

There are several steps required in the as-built modeling process. First, X-ray CT characterizes the fully assembled part. Next, image processing tools are used to perform segmentation, or definition of edges and associated volumes in the part. For the reference standards, for example, the segmentation steps included thresholding then applying erosion, dilation and median filters

using 3x3x3 voxel kernels. After segmentation, a triangulated 3D surface is generated from the segmented slices using the marching cubes algorithm [Lorensen, *et al.* 1987]. This surface consists of thousands of nodes and even more triangular elements, and represents the surface created from the voxel segmentation. In the next step, the surface is smoothed, reducing the number of triangular elements and minimizing voxel-level noise from the X-ray CT. Without this smoothing step, the number of elements in the model would be prohibitive to run an analysis. From this smoothed surface, a mesh made up of hexahedral elements was generated and fit to the surface. Different simulations may be applied to the mesh to predict the performance of the as-built object including hydrodynamic, thermal, structural and electromagnetic analyses.

## Summary

We have begun to quantitatively measure KCAT's digital radiography and computed tomography system performance. KCAT's performance has been determined for mesoscale objects (reference standards of mm extent with  $\mu\text{m}$  features). CT data has been acquired for two reference standards. The CT data from one of the reference standards has been converted to a finite element mesh that can be used for hydrodynamic, thermal, structural and electromagnetic analyses.

## Future work

- Measure CT MTFs using tube objects;
- Remeasure the DR MTFs with better edges;
- Develop quantitative data analysis techniques for 3-D CT data;
- Compare the quantitative system performance characteristics with other systems, including synchrotron and commercially available DR/CT systems.

## References

Hasegawa, B., *The Physics of Medical X-ray imaging*, Madison, WI, Medical Physics Publishing, 1991.

Logan, C., J. Haskins, K. Morales, E. Updike, J. Fugina, T. Laviertes, D. Schneberk, G. Schmid, K. Springer, P. Soltani, and K. Swartz, "Evaluation of an Amorphous Selenium Array for Industrial X-Ray Imaging", Lawrence Livermore National Laboratory, Livermore, CA, UCRL-ID-132315 (1998).

Lorensen, W. E., and H. E. Cline, "Marching Cubes: a High Resolution Surface Extraction Algorithm", *Computer Graphics*, vol. 21, n. 3, pp. 163-169, 1987.